



Tribological properties of graphite particles as an anti-friction and anti-wear additive in lithium soap grease

Shahira Liza Kamis ^{1*}, Bakhit I. Yusoff ¹, Kanao Fukuda ¹, Noor Ayuma Mat Tahir ¹, Ikmal Alif Ahmad Sukri ¹, Mohamad Ali Ahmad ²

¹ Malaysia-Japan International Institute of Technology, Universiti Teknologi Malaysia, Jalan Sultan Yahya Petra, Kampung Datuk Keramat, 54100 Kuala Lumpur, MALAYSIA.

² School of Mechanical Engineering, College of Engineering, Universiti Teknologi MARA, Shah Alam, 40450 Selangor, MALAYSIA.

*Corresponding author: shahiraliza@utm.my

KEYWORDS	ABSTRACT
Graphite Viscosity Sliding contact Friction Wear	The objective of this study is to investigate the use of graphite submicron particles as an additive to enhance the tribological properties of lithium soap grease. In this study, various concentrations of graphite particles ranging from 0 to 16 wt.% were incorporated into the lithium soap grease. The friction and wear were evaluated using a ball-on-disc tribometer, following the ASTM G99 standard. Additionally, a rheological test to measure viscosity was conducted following ISO 3219-2. The results of the experiment showed that the addition of graphite particles led to reduction in the viscosity of the lithium soap grease. Moreover, at steady-state friction, a 2 wt.% concentration of graphite resulted in a remarkable 41% decrease in the friction coefficient and a 15% reduction in wear scar diameter. These findings indicate that introducing graphite particles to lithium soap grease can significantly improve its lubrication performance, making it an effective solution to address friction and wear issues in industrial machinery.

Received 3 November 2023; received in revised form 9 January 2024; accepted 24 February 2024.

To cite this article: Kamis et al., (2024). Tribological properties of graphite particles as an anti-friction and anti-wear additive in lithium soap grease. *Jurnal Tribologi* 40, pp.179-198.

1.0 INTRODUCTION

The growing need for industrial machinery has spurred the development of specialized lubricants including the grease formulated from waste materials.(Abdu Rahman et al., 2019; Japar et al., 2020; Mohd Sofi et al., 2019; Suhaila et al., 2018).One of the functions of these lubricants is ensuring smooth operations even under tough conditions, such as high loads and low speeds (Nabhan et al., 2021). These challenging situations demand the use of the right lubricants to guarantee the machinery functions properly and efficiently (Yelatontsev & Mukhachev, 2021). Due to friction and wear issues that occur during the operation of the machine element, lubricating grease finds widespread use to prevent its direct contact (Zhang et al., 2020). Grease serves as a protective layer, maintaining a steady lubricating film to keep the machinery running smoothly and prolong its lifespan (Zhang et al., 2020) . As of today, aluminium-based grease, calcium-based grease, and lithium-based grease are the most used and selected lubricant due to their wide range of operational temperatures, withstand loads, protection of the bearing from rust, and extension of the bearing life (Nabhan et al., 2021; Yelatontsev & Mukhachev, 2021). Since lithium-based grease is considered the ideal machine oil due to its excellent tribological properties, providing both high lubrication and high temperature capabilities, the performance of lithium-based grease is significant to enhance the long-term durability and dependability of numerous mechanical equipment. (Lin et al., 2020; Razavi et al., 2022; Wang et al., 2022; Zhang et al., 2018). Multiple techniques can be undertaken on the lubricant design to modify the grease properties by changing the base oil viscosity or adding additive (Zhang et al., 2020).

Recently, incorporating solid lubricant such as graphite, hBN (hexagonal boron nitride) or MoS₂ (molybdenum disulphide) has been introduced to improve the grease properties regarding friction reduction, anti-wear, and extreme pressure behavior. (Baş et al., 2022; Czarny & Paszkowski, 2007; Kumar et al., 2023; Larsson et al., 2021; Lee et al., 2009; Mohd Nasir et al., 2021; Sahoo & Biswas, 2014; Torres et al., 2022; Wu et al., 2023). Graphite structure consists of a succession of layers parallel to the basal plane of hexagonally linked carbon atoms. Thermodynamically, this is a stable structure or allotrope of carbon at high temperature. For lubrication properties, graphite often used due its layered structure, which allows for easy sliding of these layers against each other (Nyholm & Espallargas, 2023). When immersed in lithium soap grease, graphite can form a protective layer between contacting surfaces, making it an effective lubricant in various mechanical systems. The research conducted by (Zhang et al., 2020) found that using 2wt% of graphite as an additive in grease has significantly improved the tribological properties in terms of friction coefficient by 27% of reduction as compared with pure grease. This finding was also supported by (Chen et al., 2022), which demonstrated 2 wt.% graphite to the grease displayed in the lowest value of friction coefficient. This study however mainly focused on nano size.

Despite, it is well-acknowledged that, in the context of lithium soap grease, the acceptable upper limit for nano-sized additives is limited to less than 5 wt.% according to (Kumar et al., 2023; Wu et al., 2023). Nevertheless, the extent to which the saturation of sub-micron particles was still undebated. A study showed that nano and sub-micron sized additives are extensively used possess remarkable characteristics, including a small size effect, larger specific surface, and higher surface energy (Sharma et al., 2019).However, few studies stated that the presence of sub-micron particles promoted not much effect towards the friction enhancement. For example, a study by (Kumar et al., 2020) demonstrated that incorporating 4 wt.% of both 50 nm nano particles and 450 nm graphite particles in lithium soap grease led to substantial of grease without additives. In fact, sub-micron particles could improve the coefficient of friction up to 51 % On the other hand,

research (ref) (Nagare & Kudal, 2018) has been conducted out by introducing the 500 nm (5 wt.%) to reduce the wear, The result showed that the wear has been reduced 23.16 % by as compared to the lithium soap grease without additive. These findings played a crucial role in guiding our decision regarding particle size and concentration, emphasizing their significance in modifying the lubricating properties of lithium-soap grease, particularly on the friction and reduction.

To address this gap, the choice of 400 nm particles in the current study examined the use up to 16 wt.% of sub-micron particles in lithium soap grease to pinpoint the saturation point for graphite particles addition (Menezes et al., 2012, 2013). Therefore, graphite was chosen to be used in this study due to its relatively low cost, environmentally friendly and good performance. (Kumar et al., 2020; Niu & Qu, 2018, Sun et al., 2020, Torres et al., 2022). Thus, the aim of this study is to investigate the performance of sub-micron graphite particles as anti-friction and anti-wear using a ball on disc setup. The study involves the observation of phenomena related to the coefficient of friction and wear. This observation is conducted through spatiotemporal mapping to explain the distribution of grease (Fukuda et al., 2015; Fukuda & Morita, 2013; Yap et al., 2022) and graphite within modified grease. This distribution of graphite serves to reduce friction and act as a protective boundary layer, thereby preventing direct metallic contact during sliding. Hence, spatial temporal mapping (SMA) as insights that could serve as reference solution to address friction and wear issues in industrial machinery.

2.0 EXPERIMENTAL PROCEDURE

2.1 Properties of Lithium Soap Grease (LSG)

The base grease used in this study was commercially available multi-purpose ie; lithium soap grease (GM2) provided by bearing manufacturers (manufacturer NSK, Japan). The detailed properties of the grease lubrication are shown in Table 1 (NSK data sheet) and Table 2 (Spectroil Q100).

2.2 Preparation of the Modified Grease

Graphite particles purchased from ACS MATERIAL, USA, were chosen as additives without further purification. The characterization of graphite particles was done by Scanning electron micrographs (SEM) on graphite particles. Figure 1 shows graphite in the form of a powder with an average size of 400 nm.

Table 1: Properties of lithium soap grease.

Properties	
NLGI grade	2
Appearance	Yellowish brown
Base oil	Mineral oil
Thickener	Lithium soap
Dropping point	207°C
Service temperature range	-20~120°C

Table 2: Elemental of lithium soap grease.

Elemental composition
Lithium (Li), silicone (Si), phosphorus (P), arsenic (As), zirconium (Zr), cerium (Ce), nickel (Ni), sodium (Na), magnesium (Mg), calcium (Ca), bismuth (Bi), indium (In), iron (Fe), potassium (K), zinc (Zn), manganese (Mn), tin (Sn), vanadium (V), copper (Cu), aluminum (Al), cadmium (Cd), barium (Ba), lead (Pb)

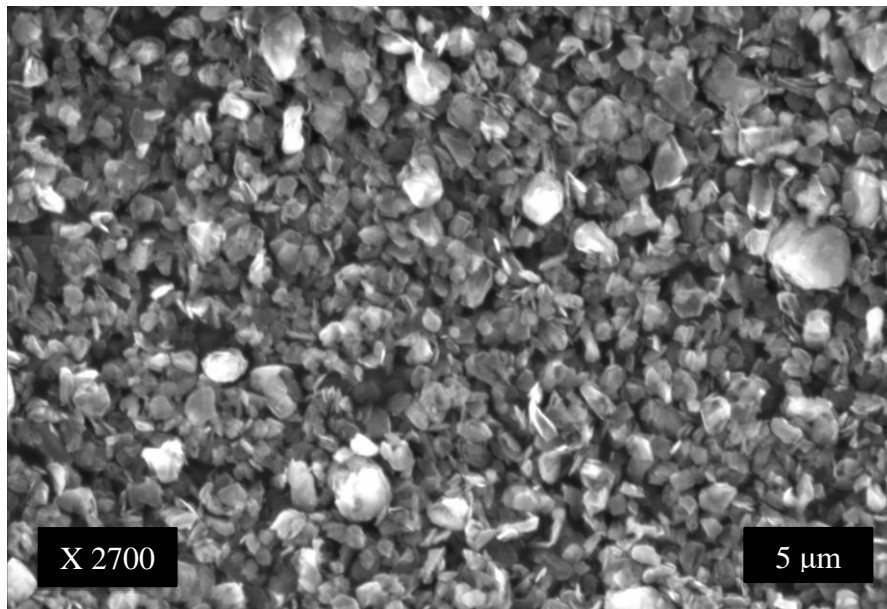


Figure 1: Surface morphology of graphite particles (average size 400 nm).

Figure 2 depicts the diagram illustrating the preparation of grease-mixed graphite particles. Firstly, the LSG (10g) was preheated up to 90°C until it reached a liquid-like and manually stirred by using a silicone stirrer to open the fibrous structures of the grease (2 minutes) before 1-16 wt% (direct mixing method) of graphite particles were added. Then, a magnetic hotplate stirrer (Kumar et al., 2023) was utilized for mixing the modified grease obtained at 300 rpm continuously within the temperature range between 80 to 90°C to ensure the modified grease homogenous distribution within the grease matrix. Lastly, the modified grease was then allowed to cool at room temperature (30 minutes) (Ahmed et al., 2020; Padgurskas et al., 2023).

Table 3 shows the detailed composition of all grease samples. Besides, the physical observation of the grease has been shown in Figure 3 where samples (a) and (b) are lithium soap grease and modified lithium soap grease with graphite particles. The presence of graphite additives has been found in the grease due to the changes in the color from yellowish to black as shown in Figure 3 (b).

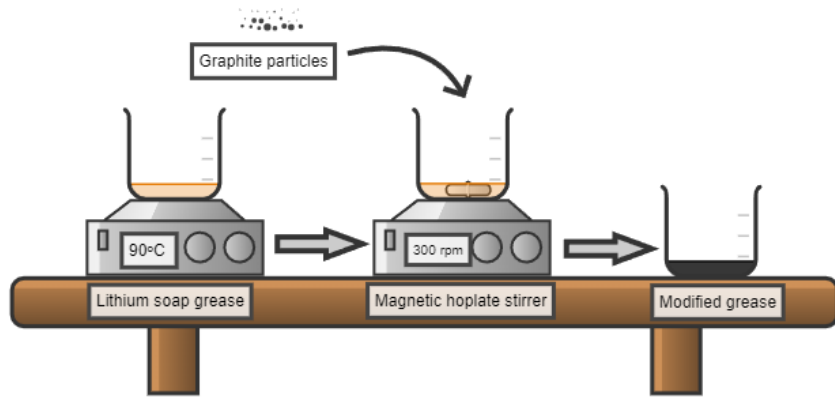


Figure 2: Diagram of the preparation for grease lubrication.

Table 3: Composition of all grease samples.

Samples	Composition (wt%)	
	Grease	Graphite
LSG	100	0
LSG-1	99	1
LSG-2	98	2
LSG-4	96	4
LSG-8	92	8
LSG-16	84	16

2.3 Grease Characterization

The grease structure of LSG in Figure 4 and modified LSG were investigated through scanning electron microscopy (SEM) (Kumar et al., 2020). To prepare the grease samples, hexane was slowly added several times to remove oil (Larsson et al., 2021). The grease samples remaining on the glass slide after oil removal displayed a white powdery appearance. Each grease type was placed on a separate disc. Then, the grease samples were sputter coated with Au/Pd to enhance the conductivity before the SEM analysis. The SEM analysis was performed with an electron acceleration voltage of 5 kV.

Furthermore, to verify the presence of graphite particles in the modified grease, Raman spectroscopy URaman-M (Technospex Pte Ltd., Singapore) at wavelength 532 nm was employed. In Raman spectroscopy, the G peak is often attributed to graphite-like structures of sp^2 sites, and the D band is related to the disorder of the graphitic structure. Much earlier research has found that the G peak shift, D peak shift, and D peak intensity in Raman spectra can give some information regarding the structure of the graphite.

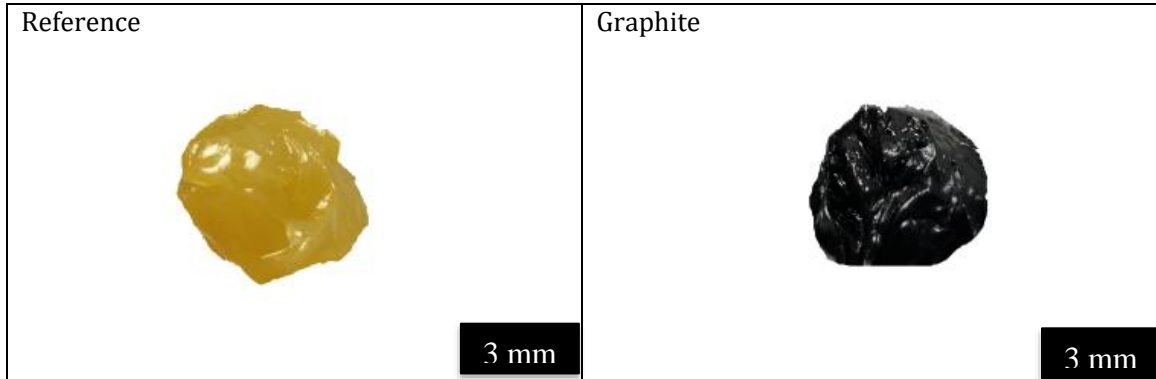


Figure 3: Images of the prepared grease samples. (a) Lithium soap grease, and (b) Modified lithium soap grease with graphite particles (Gr).

2.4 Rheological Properties of Greases

The experiment has investigated the base oil viscosity of lithium soap grease with different graphite concentrations. The rheological properties of the grease were studied using rheometer (MCR302, Austria) in rotational mode with a parallel plate PP20 with according to ISO 3219-2. The detailed experiment setup as shown in Table 4.

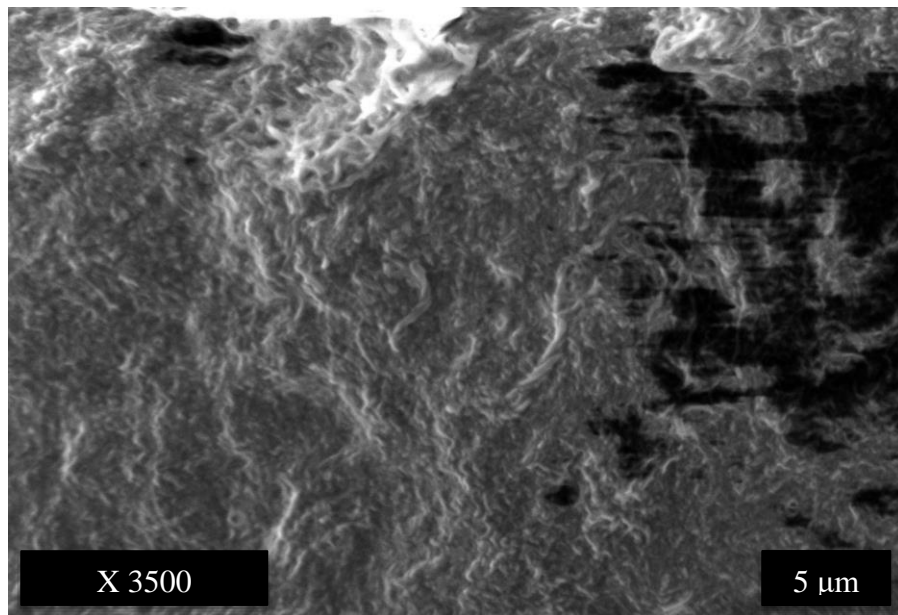


Figure 4: SEM images of the thickener microstructure for the following base greases: LSG without graphite particle reference thickener.

Table 4: Rheological experiment details.

Parameter	Value
Temperature	25°C
Shear rate	0.01 – 1000 s ⁻¹
Parallel plate	PP20

2.5 Tribological Performance of Greases

2.5.1 Substrate Materials

S45C was used in this study was selected due to its good weldability, high hardness, and moderate price. It is a common material for production of machine elements such as roller bearing, piston -ring system and gears. The material with 25 mm diameter was purchased from Misumi Malaysia Sdn. Bhd. The thickness was 5 mm and there was a 4 mm hole at the center. Afterwards, the substrate with dimension 25 mm (diameter) and 5 mm (height) carbon steel was grind and polished to obtain a surface roughness, $R_a \leq 0.08 \mu\text{m}$ before it is ready for the experimental work. The counterpart ball with 8mm diameter made of SUJ2 also polished to obtain a surface roughness, $R_a \leq 0.04 \mu\text{m}$. The grease lubricating used was LSG and the modified LSG (1- 16 wt.% of 400 nm graphite particles).

2.5.2 Tribological Test

The friction coefficient of the modified LSG was evaluated using ball-on-disc tribometer according to ASTM G99 and compared to the reference, lithium soap grease (LSG). The tribological testing parameters are shown in table 5.

The normal load was applied vertically to the ball as shown in figure 5(a). A high chrome steel, SUJ2 (59-61 HRC) with an 8 mm diameter and surface roughness of 0.1- 0.24 μm and the disc is medium carbon steel, S45C was used. The contact type in this experiment is considered a non-conformal contact type. In contrast, non-conformal contact present in roller bearings and gears results in high contact pressure between 1 to 4 GPa. The contact type in the experiment is considered non conformal as the tribo-tester used has sphere-on-plane configuration. Besides that, the selected normal load 10 N which corresponds to 1.17 GPa estimated contact stress respectively is used to evaluate an effectiveness of grease at a constant speed of 100 rpm. In this study, only sliding behavior is considered. For lubrication, approximately 0.5 g of grease was evenly applied to the contact area of the disc for each test. In actual practice, the distribution of the grease is controlled by the grease.

Table 5: Tribological experiment details.

Parameter	Value
Sliding velocity, v	0.1047 ms ⁻¹
Normal load, F	10 N
Number of rotations	6000
Temperature	25°C
Lubrication	LSG and Modified LSG
Duration	60 mins

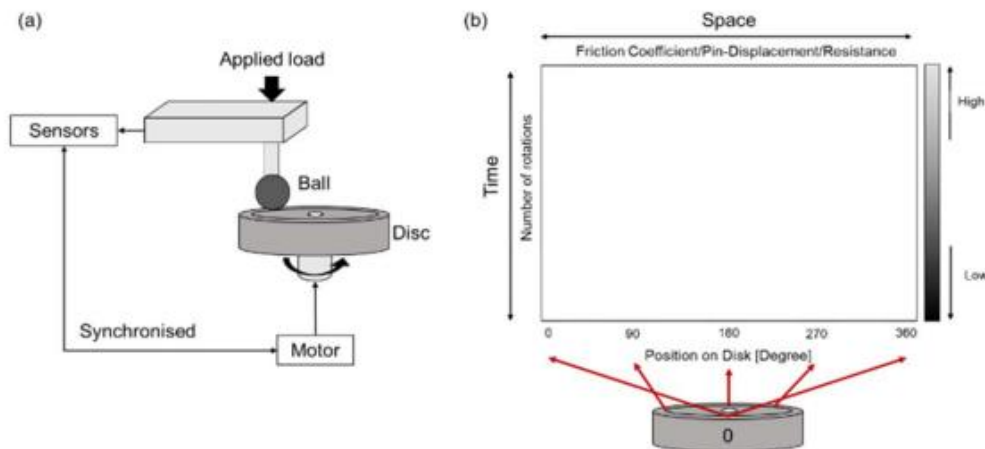


Figure 5: (a) Schematic setup of ball on disc (b) Example of SMA of tribo-data.

This study implemented spatiotemporal mapping analysis (SMA) technique, a 3D visual representation of data to pronounce the phenomena that occurred at the contact during sliding. From the results of the ball-on-disc setup used in this experiment, the x-axis represents the position on the wear track of a disc, the y-axis represents the number of sliding rotations, and the z-axis represents the magnitude of the tribo-data (friction coefficient or vertical pin position or electrical contact as presented in figure 5(b) referred to (Yap et al., 2022).

After the tribological test was done, the worn surface was characterized using HIROX Digital Microscope KH-8700. The wear scar diameter on the ball was observed to understand the effects of the grease with varying graphite concentrations on reducing wear.

3.0 RESULTS AND DISCUSSION

3.1. Characterization of Graphite in Grease

Comparative Raman spectra obtained for the LSG and modified LSG with graphite are illustrated in Figure 6. The observed Raman spectra confirmed the presence of graphite over the LSG. This verifies the graphite presence in the LSG. The typical Raman spectra for the graphite are commonly characterized by the G peak around 1580 cm^{-1} and D peak around 1350 cm^{-1} . Based on the graph, the lithium soap molecules revealed a sharp peak at 683 cm^{-1} and 1353 cm^{-1} correspond to LSG (Kumar et al., 2023). Besides, the G peak position was revealed to be shifted towards a higher wavenumber as the concentration of graphite increase up to 4 wt.%. The G peak position shifted from 1576 cm^{-1} to 1589 cm^{-1} , and the D peak intensity also increased. However, as the graphite concentration reached 8 to 16 wt.%, the G peak position shifted from 1576 cm^{-1} to 1600 cm^{-1} , and the D peak intensity also increased. This suggests that the graphite particles may have reached its saturation concentration. Overall, it can be concluded that graphite particles were dispersed in the lithium soap grease.

Further study was conducted on modified LSG with 16 wt.%. The SEM imaging results are displayed in Figure 7a and b show for the graphite particle before and after mixing with LSG, respectively. As shown in figure 7d, the elemental mappings of graphite particles appear to be

uniformly distributed when mixed. Dots maps confirmed the presence of graphite particles and indicated a better quality of dispersion.

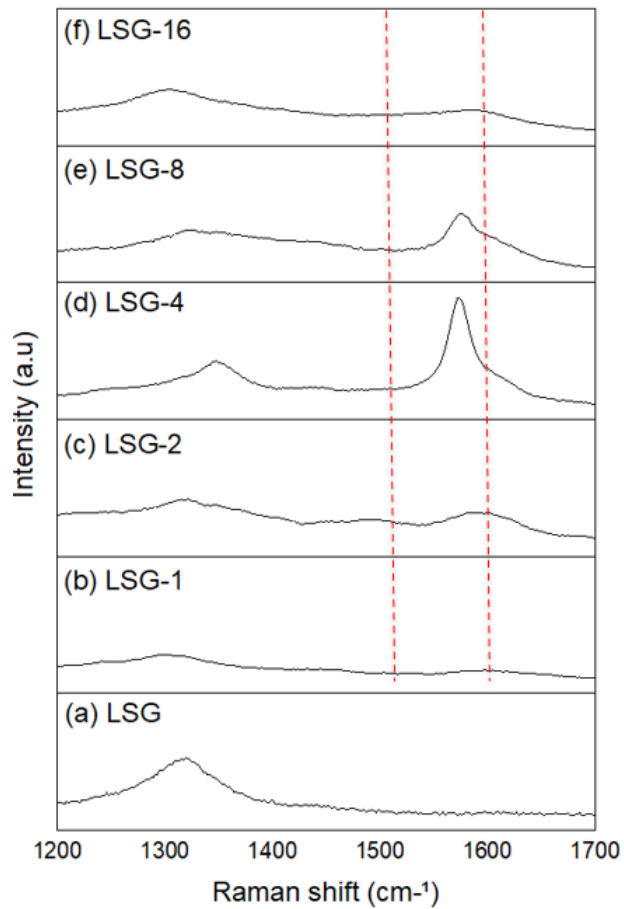


Figure 6: Raman Spectra on (a) LSG and (b) to (f) modified LSG with different graphite concentration.

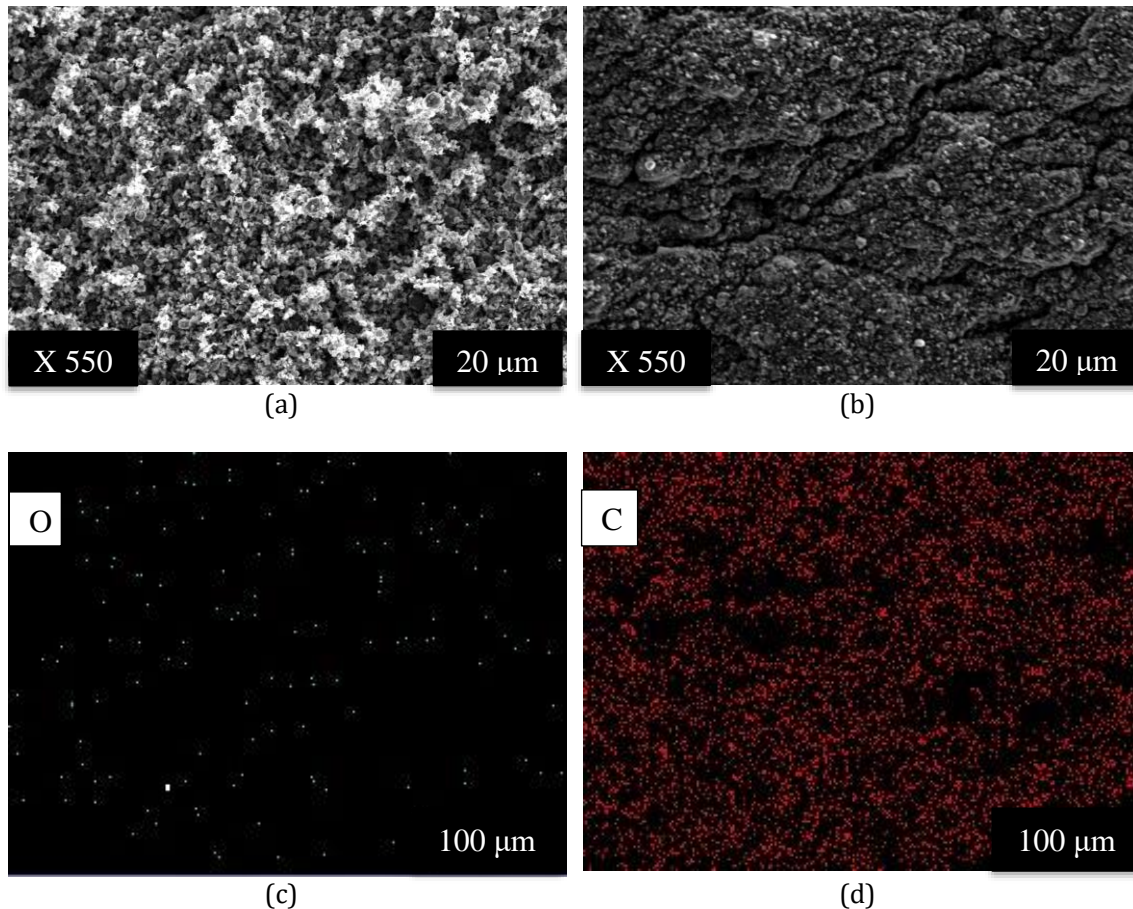


Figure 7: (a) graphite in the form of a powder (b) modified graphite with 16 wt.% (c) oxygen element mapping from image b (d) carbon element mapping from image b.

3.2 Dynamic Viscosity of The Grease

Adjacent fluid layers are responsible for viscous friction and viscosity of modified LSG can determine the shearing force between these layers (Kotia et al., 2018). Based on the observation in Figure 8, all the samples depict the shear thinning phenomenon with a shear rate under the motion state of shear rate from 0.01 s^{-1} to 1000 s^{-1} at a temperature of 25°C . The presence of graphite particles will disrupt the fluid, and the primary cause of the apparent viscosity decrease at higher shear rates is the dynamic interactions between particles. In general, no measurable change in viscosity is observed at high shear strain, indicating that well dispersed graphite does not affected viscosity under high shear conditions.

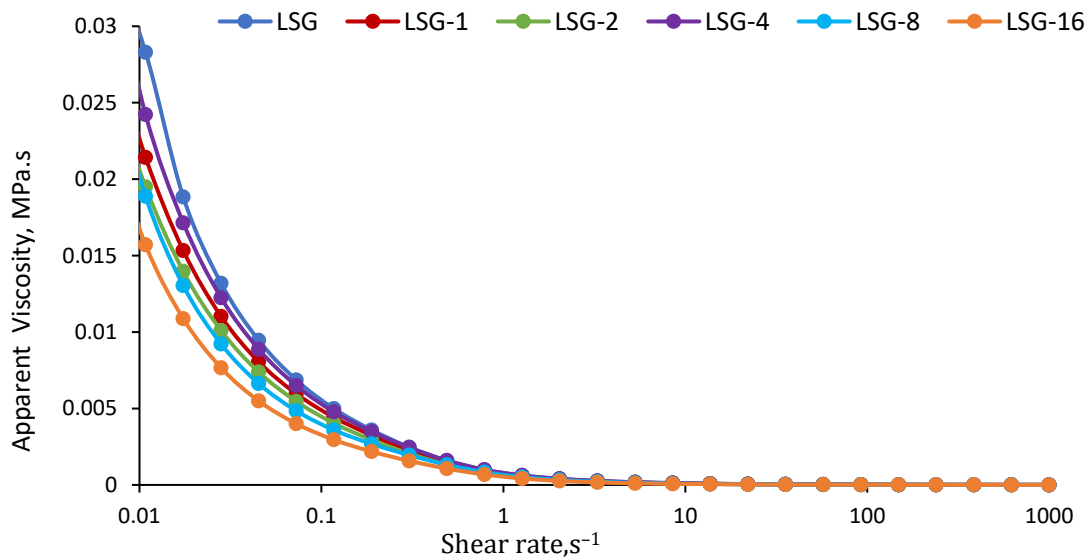


Figure 8: Variation of apparent viscosity with the shear rate for the lubricating greases.

Findings show that LSG has higher apparent viscosity, followed by LSG-4, LSG-1, LSG-2, LSG-8, and LSG-16. The lithium soap fiber in LSG exhibited a sharp peak at 683 cm⁻¹ and 1353 cm⁻¹ correspond to LSG (Kumar et al., 2023) compared with modified LSG. Therefore, lithium thickener has a strong three-dimensional network held together by van der Waals which contributes to immobilizing the base oil and increasing the base oil viscosity. (Czarny & Paszkowski, 2007).

By adding graphite, LSG has shown in reducing base oil viscosity. It is believed that graphite caused more random internal friction among the particles which generate heat during mixing process modified LSG, thereby weak the mesh structure including Van der Waals and hydrogen bonds tends to break up and become difficult in holding base oil in the grease matrix. As a result, the phenomenon led to the reduction of viscosity. Meanwhile, the viscosity of LSG-4 increased and suggested film thickness is dominated by lithium soap thickener at boundary to reach on the metal surface which viscosity significantly increase (Larsson et al., 2021). This can be proven where the Raman spectroscopy in figure 6 of LSG-4 shows the obvious peak of graphite. However, the reason behind these phenomenon remains unclear.

Figure 9 depict the structure of LSG and modified LSG when adding graphite particles thereby particles tend to break up the fibrous structure. According to the analysis, the addition of graphite particles was added up to 16 wt% to purposely reach the sites on the metal surfaces (Naveira Suarez et al., 2010). Graphite's layered structure makes it easy to slide and to act as a protective boundary film. Therefore, the findings shows that the addition of graphite up to 16 wt.% won't significantly alter the function of the lithium soap as thickeners but it is suggested that the reduction in viscosity due to disentanglement of the fibrous structure and graphite particles successfully reach the surfaces on the metal surfaces, respectively (Jablonka et al., 2013; Sadeghalvaad et al., 2019).

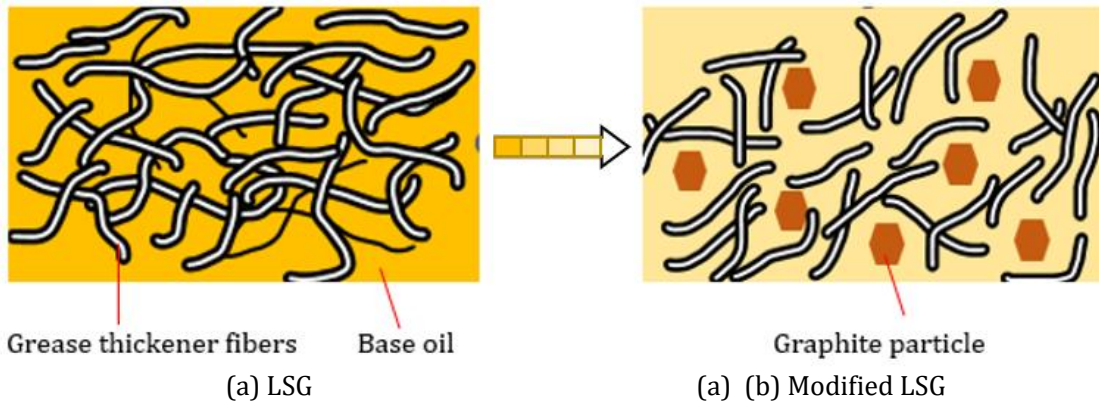


Figure 9: Illustration of the structure in (a) LSG and (b) modified LSG. (The background colors indicate the viscosity level of the samples less viscous).

3.3. Friction Coefficient for Reference LSG And Modified LSG

Figure 10 shows the friction coefficient behavior of the LSG with varying with respect to sliding number at 10 N. The friction behavior can be divided into two stages of running in period and steady state (Basir et al., 2023). At running in period, LSG, LSG-1 and LSG-4 exhibited a noticeable friction peak within the first 2000 rotations compared to other modified LSG.

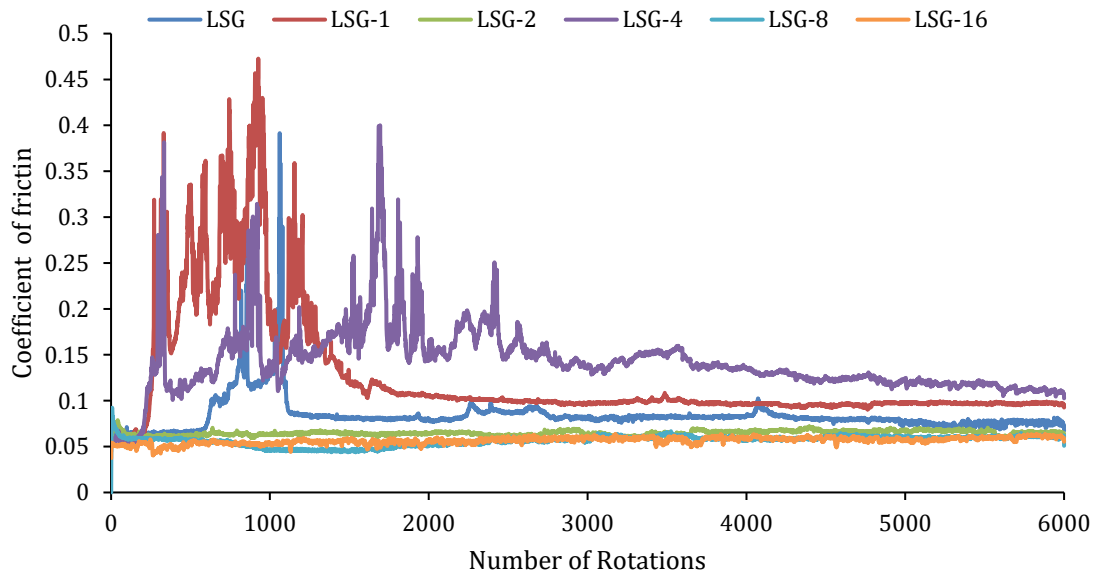


Figure 10: Friction behavior of the surfaces in 6000 cycles under 10 N load.

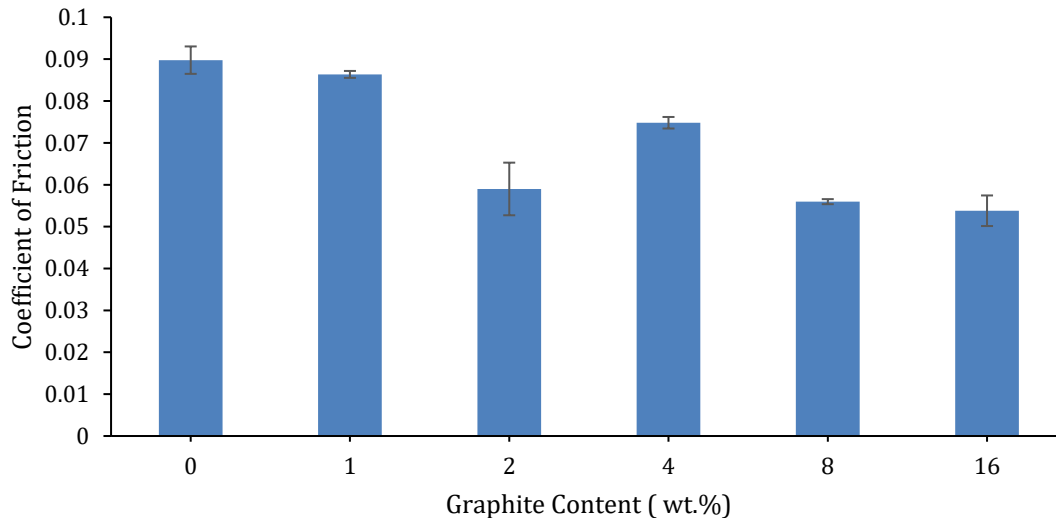


Figure 11: Average coefficient of friction (COF) against lithium soap grease containing graphite at different concentrations.

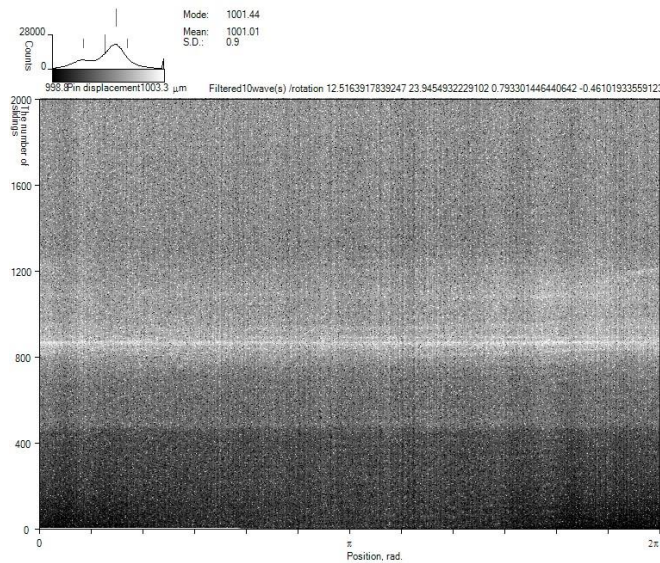
In the next stage from 3200 to 6000 rotations, the friction coefficient reached a steady state in which adhesion and wear debris play main roles. At this moment, the average values of the friction coefficient were obtained and measured. From the graph, LSG-2 and LSG-8 achieved the lowest average coefficient (COF) of 0.0593 and 0.0560, respectively followed by LSG-16 (0.054). This reduction in friction suggests that graphite effectively reached the metal surfaces and functioned as ball bearings to prevent contact. (Lee et al., 2009).

Based on the result, it observed that LSG -2 shows the optimal concentration in reducing COF. This phenomenon can be attributed to the stacked layered of graphite particles, which are held together by weak van der Waals forces, resulting in low shear and easy to slip of adjacent layers (Wu et al., 2023). It is hypothesized that, during the friction process, graphite particles might be reach the metal surfaces and deposited on the rubbing surfaces, forming a boundary film (Chen et al., 2022, Ji et al., 2011). However, similar trends were observed in the viscosity and COF for LSG-4. The COF, also recorded as 0.0748, increased in a manner resembling the rise in base oil viscosity. This suggested that behavior of LSG-4, may be attributed to the lithium thickener retaining the base oil, preventing it from shearing out and leading to the formation of thicker film, primarily due to dominant role of the lithium thickener (Sun et al., 2020). According to the above analysis, LSG-2 is the optimal concentration that can improve the friction behavior of lithium soap grease corresponding to the low base oil viscosity and stable graphite concentrations. To study the effectiveness of LSG with the distribution of graphite particles. The spatial temporal mapping was used to explain the phenomenon and focused on LSG-8 since it has the least fluctuation of the error bar.

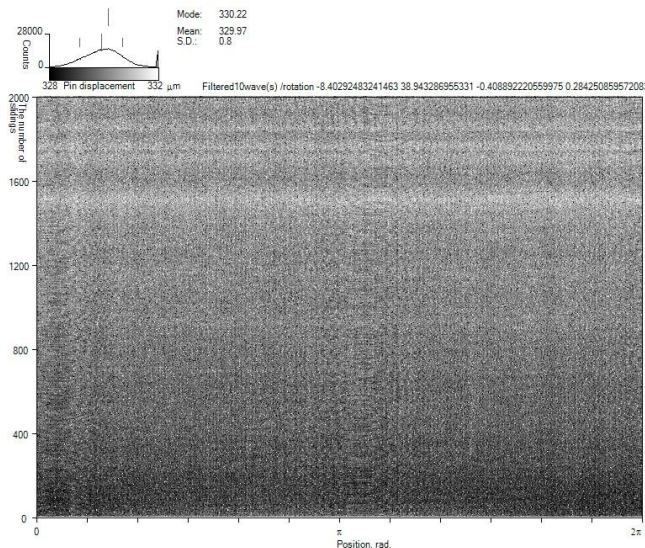
3.4 SMA for reference LSG and selected modified LSG.

This phenomenon can be proven by observing the vertical pin displacement behaviour and contact voltage during the sliding from SMA in figure. To understand the SMA if pin-displacement behaviour, intensity indication for the tribo-data is used where the darker colour indicates low

pin displacement while brighter colour indicates high pin displacement as shown in figure 12 and Figure 13.



(a) LSG



(b) Modified LSG

Figure 12 SMA of pin displacement (a) LSG (b) modified LSG in 2,000 cycles under 10 N load. Note: SMA is filtered to remove the disc's misalignment.

Findings show that low pin displacements for LSG at initial 500 rotations which indicates a thin layer film of grease help to protect the surface during sliding. However, at 600 rotations the pin displacement increases undergo running in period and indicates adhesive grew on the pin until 1200 rotations. Afterward, the grease achieves steady state condition where the pin

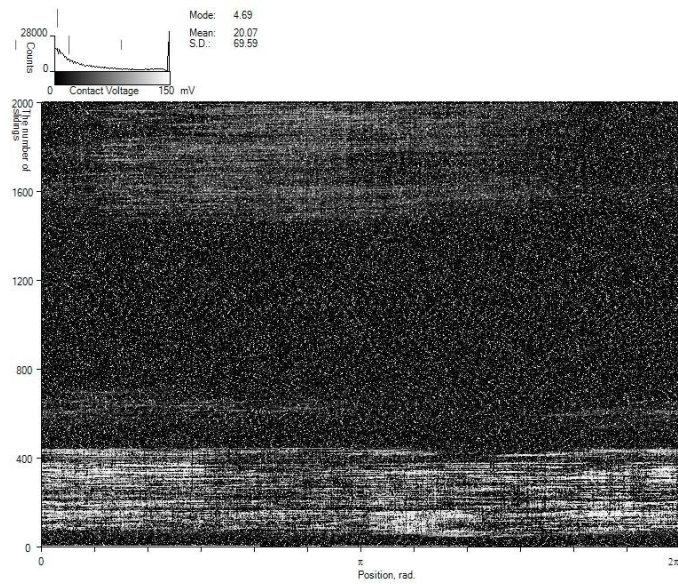
decrease indicates the adhesive substance or wear particle from pin which might transfer to disc (Fukuda & Morita, 2013). A horizontal band of high pin displacement results in low friction and low pin displacement resulted in high friction.

Besides the SMA, modified LSG shows moderate pin displacement while increases in the sliding number presented in figure 12(b). It is suggested that presence of graphite particles in lithium soap grease which functioned as a ball bearing (Lee et al., 2009) during sliding to prevent direct contact. A horizontal band of high pin displacement indicates formation of graphite particles transfer film build up which result in low friction.

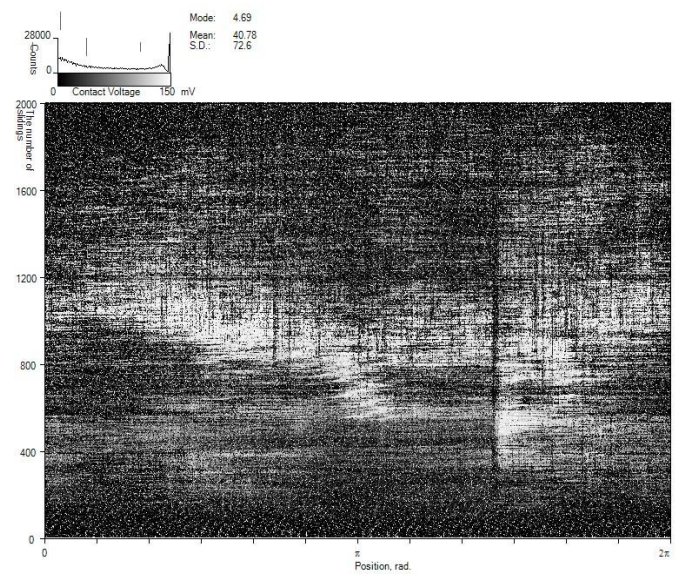
Furthermore, SMA contact voltage behavior, intensity indication for the tribo-data is used where the darker colour indicates metal to metal contact while brighter colour indicates presence of lubricants as shown in Figure 13.

Findings show that LSG at initial 500 rotations which indicates a thin layer film of grease help to protect the surface during sliding. However, at 600 rotations the grease pushed away and the darker colour in horizontal indicate the metal-to-metal contact. Afterward, accumulation of debris will mix with the left-over grease which indicates the steady state condition where the COF becomes stable at average 0.095.

However, modified LSG shows the brighter colour which it is suggested that there is the presence of graphite particles in lithium soap grease which suggested due to uniform graphite particles distributed that prevent direct contact of surface during sliding. A horizontal band of modified LSG indicates the distribution and formation of graphite particles transfer film build up helps during sliding resulted in low friction at average 0.0560.



(a) LSG



(b) Modified LSG

Figure 13 Figure 2 SMA of contact voltage (a) LSG (b) modified LSG in 2,000 cycles under 10 N load. Note: SMA is filtered to remove the disc's misalignment.

3.4 Wear Properties for Reference LSG and Modified LSG

Figure 14 displays the wear scars of the tested steel balls after a 60-minute run time using lithium soap grease containing graphite. In Figure 15, we can observe the average diameters of the wear scars at eclipse (horizontal) measured from three trials.

Further, the impact of the graphite concentration on the average WSD of steel balls is also obvious. Notably, the sizes of the wear scars decreased as the graphite concentrations at 2 wt.%. This can be justified during the friction process; graphite particles are incorporated into the grease and deposited on the worn surface, forming a lubricating layer that fills the irregularities of the rough surface, resulting in a smoother contact area (Wu et al., 2023) (Niu & Qu, 2018). However, LSG-4, LSG-8 and LSG-16, the wear scars showed increasing and lead to severe wear. This behavior might be due to the formation of layers that break away which results in higher wear due to third body wear (Naveira Suarez et al., 2010b). Therefore, the anti-wear ability becomes worse with increasing graphite particle. According to the above analysis, LSG-2 has the best durability with low WSD.

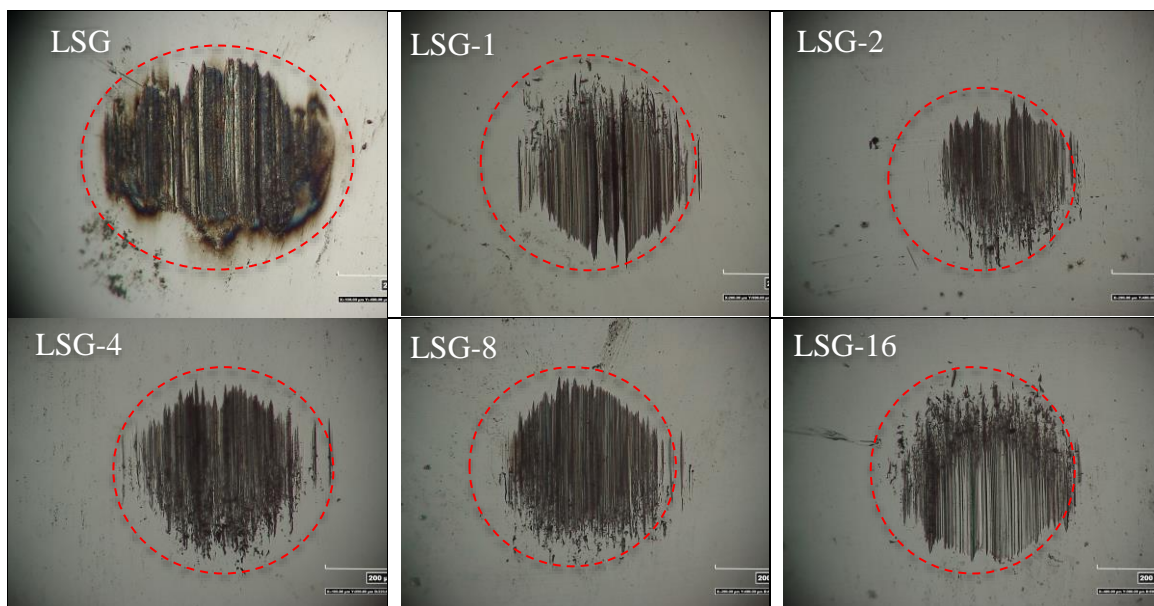


Figure 14: The wear scars on steel balls lubricated with LSG containing varying concentrations of graphite were observed and analyzed.

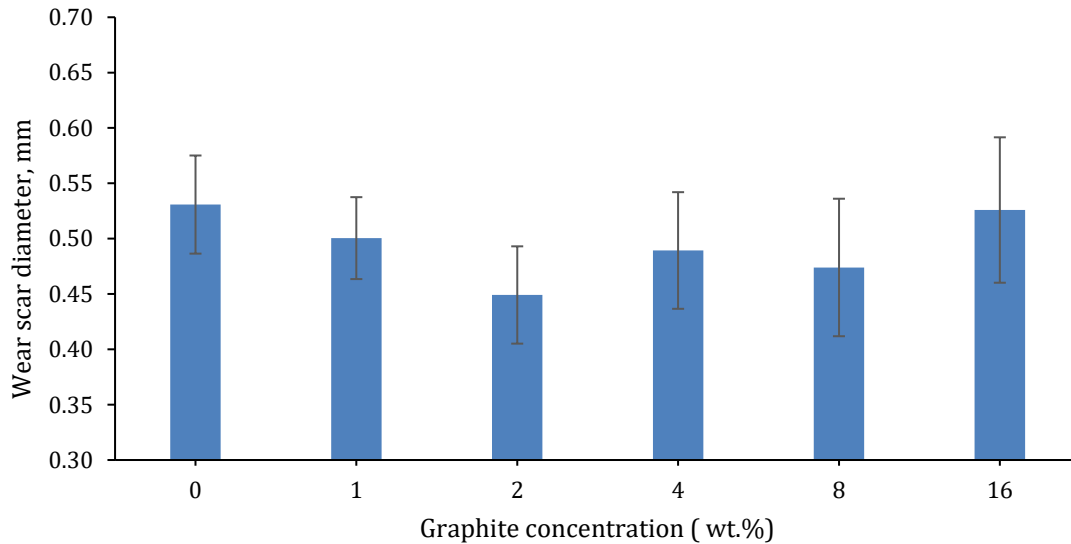


Figure 15: Average wear scar diameter of steel balls lubricated with LSG containing graphite at different concentrations.

CONCLUSIONS

In conclusion, the utilization of graphite particle (SM) in the LSG successfully enhanced the viscosity, friction coefficient and wear scar diameter. LSG-2 demonstrated the most significant improvements, with remarkable reductions of 41% in COF and 15% in WSD, respectively. It was shown that the additive delayed the deformation of the LSG when shear strain was applied. The study demonstrated that 2 wt.% concentration of graphite particles enhances the tribological performance of LSG. The excessive concentrations have a minor effect on the overall viscosity and COF. However, the excessive concentration deflects the wear scar which increased significantly. The result highlights the concentration of graphite particles as a key factor influencing viscosity and tribological properties (friction and wear). Future research should focus on investigating the mechanisms and effect of polarization between thickener and additives on the rheological and tribological properties of LSG.

ACKNOWLEDGMENT

This study was funded by NSK Ltd Co through Grant No. R.K130000.7343.4B661.

REFERENCES

- Abdu Rahman, N. W., Japar, N. S. A., Aziz, M. A. A., Razik, A. H. A., & Yunus, M. Y. M. (2019). Sodium grease formulation from waste engine oil. *IOP Conference Series: Earth and Environmental Science*, 257(1). <https://doi.org/10.1088/1755-1315/257/1/012018>
- Ahmed, E., Nabhan, A., Ghazaly, N. M., Abdel-Jaber, G., & El Jaber, A. G. (2020). Tribological Behavior of Adding Nano Oxides Materials to Lithium Grease: A Review View project An

- analytical method for solving exact solutions of the convective heat transfer in fully developed laminar flow through a circular tube View project Tribological Behavior of Adding Nano Oxides Materials to Lithium Grease: A Review. *American Journal of Nanomaterials*, 8(1), 1–9. <https://doi.org/10.12691/ajn-8-1-1>
- Basir, A., Liza, S., Fukuda, K., & Mat Tahir, N. A. (2023). Tribological behaviour of multi-shape photochemical textured surfaces. *Surface Topography: Metrology and Properties*, 11(2). <https://doi.org/10.1088/2051-672X/acd0c6>
- Chen, Y., Sun, X., Zhang, T., Han, C., Ye, X., Liu, X., Zhao, Y., Zhang, L., Zeng, G., & Aizaz, A. (2022). Tribological performance study of zirconium phosphate as an additive in titanium complex grease. *Materials Letters*, 321. <https://doi.org/10.1016/j.matlet.2022.132402>
- Czarny, R., & Paszkowski, M. (2007). The influence of graphite solid additives, MoS₂ and PTFE on changes in shear stress values in lubricating greases. *Journal of Synthetic Lubrication*, 24(1), 19–29. <https://doi.org/10.1002/jsl.26>
- Fukuda, K., & Morita, T. (2013). Analytical method for temporal changes in repeated sliding phenomena. *Procedia Engineering*, 68, 213–218. <https://doi.org/10.1016/j.proeng.2013.12.170>
- Hemmat Esfe, M., Afrand, M., Yan, W. M., Yarmand, H., Toghraie, D., & Dahari, M. (2016). Effects of temperature and concentration on rheological behavior of MWCNTs/SiO₂(20-80)-SAE40 hybrid nano-lubricant. *International Communications in Heat and Mass Transfer*, 76, 133–138. <https://doi.org/10.1016/j.icheatmasstransfer.2016.05.015>
- Jablonka, K., Glovnea, R., Bongaerts, J., & Morales-Espejel, G. (2013). The effect of the polarity of the lubricant upon capacitance measurements of EHD contacts. *Tribology International*, 61, 95–101. <https://doi.org/10.1016/j.triboint.2012.11.016>
- Japar, N. S. A., Aziz, M. A. A., & Hamid, N. (2020). Synthesis and properties evaluation of sodium grease formulated from used transformer oil as base oil. *IOP Conference Series: Materials Science and Engineering*, 863(1). <https://doi.org/10.1088/1757-899X/863/1/012058>
- Ji, X., Chen, Y., Zhao, G., Wang, X., & Liu, W. (2011). Tribological properties of CaCO₃ nanoparticles as an additive in lithium grease. *Tribology Letters*, 41(1), 113–119. <https://doi.org/10.1007/s11249-010-9688-z>
- Kotia, A., Rajkhowa, P., Rao, G. S., & Ghosh, S. K. (2018). Thermophysical and tribological properties of nanolubricants: A review. In *Heat and Mass Transfer/Waerme- und Stoffuebertragung* (Vol. 54, Issue 11, pp. 3493–3508). Springer Verlag. <https://doi.org/10.1007/s00231-018-2351-1>
- Kumar, N., Saini, V., & Bijwe, J. (2020). Tribological Investigations of Nano and Micro-sized Graphite Particles as an Additive in Lithium-Based Grease. *Tribology Letters*, 68(4). <https://doi.org/10.1007/s11249-020-01362-1>
- Kumar, N., Saini, V., & Bijwe, J. (2023). Dependency of Lithium Complex Grease on the Size of hBN Particles for Enhanced Performance. *Tribology Letters*, 71(1). <https://doi.org/10.1007/s11249-022-01691-3>
- Larsson, E., Westbroek, R., Leckner, J., Jacobson, S., & Rudolphi, Å. K. (2021). Grease-lubricated tribological contacts – Influence of graphite, graphene oxide and reduced graphene oxide as lubricating additives in lithium complex (LiX)- and polypropylene (PP)-thickened greases. *Wear*, 486–487. <https://doi.org/10.1016/j.wear.2021.204107>
- Lee, C. G., Hwang, Y. J., Choi, Y. M., Lee, J. K., Choi, C., & Oh, J. M. (2009). A study on the tribological characteristics of graphite nano lubricants. *International Journal of Precision Engineering and Manufacturing*, 10(1), 85–90. <https://doi.org/10.1007/s12541-009-0013-4>

- Mohd Sofi, S. N. A., Abd Aziz, M. A., Anang Japar, N. S., Abdu Rahman, N. W., Abdulhalim, A. R., & Mohd Yunus, M. Y. (2019). Preparation and characterization of grease formulated from waste transformer oil. *IOP Conference Series: Materials Science and Engineering*, 702(1). <https://doi.org/10.1088/1757-899X/702/1/012034>
- Nabhan, A., Rashed, A., Ghazaly, N. M., Abdo, J., & Danish Haneef, M. (2021). Tribological Properties of Al₂O₃ Nanoparticles as Lithium Grease Additives. <https://doi.org/10.3390/lubric>
- Naveira Suarez, A., Grahn, M., Pasaribu, R., & Larsson, R. (2010a). The influence of base oil polarity on the tribological performance of zinc dialkyl dithiophosphate additives. *Tribology International*, 43(12), 2268–2278. <https://doi.org/10.1016/j.triboint.2010.07.016>
- Naveira Suarez, A., Grahn, M., Pasaribu, R., & Larsson, R. (2010b). The influence of base oil polarity on the tribological performance of zinc dialkyl dithiophosphate additives. *Tribology International*, 43(12), 2268–2278. <https://doi.org/10.1016/j.triboint.2010.07.016>
- Niu, M., & Qu, J. (2018). Tribological properties of nano-graphite as an additive in mixed oil-based titanium complex grease. *RSC Advances*, 8(73), 42133–42144. <https://doi.org/10.1039/c8ra08109c>
- Padgurskas, J., Johns, E. I., Radulescu, I., Radulescu, A. V., Rukuiža, R., Snitka, V., Kreivaitis, R., Kupčinskis, A., & Volskis, D. (2023). Tribological study of beeswax-thickened biogrease and its modification with carbon nanoparticles. *Tribology International*, 184. <https://doi.org/10.1016/j.triboint.2023.108465>
- Sadeghalvaad, M., Dabiri, E., & Afsharimoghadam, P. (2019). Lithium lubricating greases containing carbon base nano-additives: preparation and comprehensive properties evaluation. *SN Applied Sciences*, 1(3). <https://doi.org/10.1007/s42452-019-0289-7>
- Suhaila, N., Japar, A., Aizudin, M., Aziz, A., & Razali, M. N. (2018). Formulation of lubricating grease using Beeswax thickener. *IOP Conference Series: Materials Science and Engineering*, 342(1). <https://doi.org/10.1088/1757-899X/342/1/012007>
- Sun, Z., Xu, C. ming, Peng, Y. xing, Shi, Y. yu, & Zhang, Y. wei. (2020). Fretting tribological behaviors of steel wires under lubricating grease with compound additives of graphene and graphite. *Wear*, 454–455. <https://doi.org/10.1016/j.wear.2020.203333>
- Torres, H., Podgornik, B., Jovičević-Klug, M., & Rodríguez Ripoll, M. (2022). Compatibility of graphite, hBN and graphene with self-lubricating coatings and tool steel for high temperature aluminium forming. *Wear*, 490–491. <https://doi.org/10.1016/j.wear.2021.204187>
- Wu, C., Hong, Y., Ni, J., Teal, P. D., Yao, L., & Li, X. (2023). Investigation of mixed hBN/Al₂O₃ nanoparticles as additives on grease performance in rolling bearing under limited lubricant supply. *Colloids and Surfaces A: Physicochemical and Engineering Aspects*, 659. <https://doi.org/10.1016/j.colsurfa.2022.130811>
- Yap, K. K., Fukuda, K., Vail, J. R., Wong, J., & Masen, M. A. (2022). Spatiotemporal mapping for in-situ and real-time tribological analysis in polymer-metal contacts. *Tribology International*, 171. <https://doi.org/10.1016/j.triboint.2022.107533>
- Yelatontsev, D., & Mukhachev, A. (2021). Processing of lithium ores: Industrial technologies and case studies – A review. In *Hydrometallurgy* (Vol. 201). Elsevier B.V. <https://doi.org/10.1016/j.hydromet.2021.105578>
- Zhang, J., Wang, A., & Yin, H. (2020). Preparation of graphite nanosheets in different solvents by sand milling and their enhancement on tribological properties of lithium-based grease. *Chinese Journal of Chemical Engineering*, 28(4), 1177–1186. <https://doi.org/10.1016/j.cjche.2020.01.013>